

## Recoil momentum effects in quantum processes induced by twisted photons

Andrei Afanasev<sup>1</sup>, Carl E. Carlson,<sup>2</sup> and Asmita Mukherjee<sup>3</sup>

<sup>1</sup>*Department of Physics, The George Washington University, Washington, DC 20052, USA*

<sup>2</sup>*Physics Department, College of William & Mary, Williamsburg, Virginia 23187, USA*

<sup>3</sup>*Department of Physics, Indian Institute of Technology Bombay, Powai, Mumbai 400076, India*



(Received 30 June 2020; accepted 4 March 2021; published 6 May 2021)

We consider physical processes caused by the twisted photons for a range of energy scales, including optical (eV) and nuclear (MeV). We demonstrate that in order to satisfy angular momentum conservation, absorption of a twisted photon leads to a transverse recoil of the final particle or a system of particles, leading to an increased threshold energy requirement for the reaction to proceed. Modification of the threshold energy is predicted for photoabsorption on cold trapped ions of  $^{40}\text{Ca}^+$ , along with emerging new transverse-motion sidebands, and for photodisintegration of deuterium.

DOI: 10.1103/PhysRevResearch.3.023097

### I. INTRODUCTION

Twisted photons are photons with a shaped wavefront with swirling local momentum or swirling Poynting vectors about a vortex line [1,2]. Due to the swirling wavevector, the intrinsic total angular momentum (AM) of the twisted photon along the direction of propagation is  $m_\gamma \hbar$ , where  $m_\gamma$  can be any integer. Processes initiated by twisted photons follow enhanced AM selection rules [3,4], different from plane-wave photons. These selection rules have been confirmed by experiments with cold trapped  $^{40}\text{Ca}^+$  ions [5,6].

The swirling local momentum of the twisted photon can give significant transverse momentum to the final state, as pointed out by Barnett and Berry [7,8]. Near a vortex in a monochromatic light beam, the length of the local wavevector, or local momentum, can in fact exceed the wavenumber of any of the plane waves in the superposition representing the beam. These large transverse momenta potentially impart what Barnett and Berry call “superkicks” to small particles located near the vortex, as those particles absorb light from the beam.

It has been explicitly shown in a quantum formalism of twisted-photon absorption by single atoms, that the AM that does not go into internal electronic excitations is passed to the target atom’s center-of-mass (CM) motion [9,10] due to AM conservation. Thus the superkick follows as a result of AM conservation. The existence of the superkick, which adds to the kinetic energy of the final state, must lead to a modification of the threshold energies needed for a variety of physical processes.

In the present paper, we consider the kinematics of twisted-photon absorption, on an atom or on an atomic nucleus, and in particular how the energy threshold requirements vary with the distance of the target from the photon’s vortex line. We will discuss the significance of the enhanced threshold requirements, and possible effects on the reaction cross section. We will see that in an atomic situation the superkick effect is small but potentially observable in the laboratory. The effect can become more pronounced for a nuclear process, which we will discuss.

In addition we will explicitly consider how one might observe as superkick acting on atoms held in a trap. The atom’s CM motion can be excited to a higher excitation of the confining potential. The calculated excitation probability is not large except at small impact parameters, but is potentially observable. The size of the transition probability depends partly on how tightly the atom is confined. The atom itself is small relative to the wavelength of visible light twisted photons, but the size that matters is the scale of the confinement region in the trap that is holding the ion in place. That means that the relevant atomic size scale is of the order of tens of nanometers rather than tenths of nanometers. Nonetheless, the confinement region appears small enough to see an effect, as we shall argue below. The ion is trapped and the superkick will not free it, but the kick can push the ion into a higher level in the potential with visible consequences.

Regarding the impact parameters, as one approaches the vortex line, the density of the photon state decreases. However, the local momentum relative to the probability density in the same region can get very large. There is thus a region where densities are very low and the momenta very high. A sufficiently small probe, for example the ion, fitting in this region may interact rarely but on interaction will receive a lot of transverse momentum; in some circumstances, considerably more than the longitudinal momentum of the Fourier components of the twisted photon. Hence the name “superkick.”

Superkicks, as already noted, can occur because of interference effects that allow the local wavenumber to be larger than

the wavenumber of any of the Fourier modes representing the beam. Superoscillations are a related phenomenon, wherein interference effects allow a light beam in certain regions to have a wavelength arbitrarily shorter than any of the Fourier components of the wave (for a review see [11]). Superkicks and superoscillations share the feature of occurring where the probability amplitude has small magnitude, though this is not the crucial feature here.

Crucial is that superoscillations are experimentally seen, and are coming under sufficient control to be used in biological microscopy (see, for example, [11–13]). The short wavelengths produced by superoscillation allows exceeding classical diffraction limits on resolution by large margins. Again, in the case of superoscillations, this is not just calculation but observation. If superoscillation phenomena can be observed, superkicks should also exist and be observable. Evidence should be sought, and the present paper does contain useful suggestions.

Other novel kinematic effects in collisions of twisted particles have been recently discussed [14,15]. Throughout the paper, we use units where  $\hbar = c = 1$ .

## II. KINEMATICS OF TWISTED-PHOTON ABSORPTION

### A. Angular momentum conservation and a superkick

Let us consider an atom or a subwavelength-size target that absorbs a twisted photon; the target is located at a distance  $b$  away from the photon's axis, as shown in Fig. 1. The formalism for calculating individual quantum transition amplitudes due to absorption of the twisted photons can be found elsewhere [3,4,16]; here, we are concerned with the magnitude of recoil momentum  $p_T$  of the target after photoabsorption.

The transverse kick given to a target atom offset distance  $b$  from the vortex line of the photon relates directly to the AM transferred to the atom's overall center of mass. Hence, we start by considering the average angular momenta given to the internal electronic state and to the atomic c.m. in a photoexcitation process.

The expectation value  $\langle \ell_z \rangle$  of AM transferred by a twisted photon with AM  $z$ -projection  $m_\gamma$  to internal degrees of freedom of an atom can be expressed, in terms of the probabilities  $w(m_f)$  for exciting the atom to states with magnetic quantum numbers  $m_f$  [17,18] as

$$\langle \ell_z \rangle = \sum_{-\ell < m_f < \ell} m_f w(m_f). \quad (1)$$

Our interest here is in the residual, the part of the initial AM not transferred to the internal excitation, which goes to the atom's c.m. motion [10]. From AM conservation,

$$\langle \ell_z \rangle_{\text{c.m.}} = m_\gamma - \langle \ell_z \rangle. \quad (2)$$

Plots of AM transfer  $\langle \ell_z \rangle_{\text{c.m.}}$  versus impact parameter  $b$  are shown in Figs. 2 and 3. Details of how the calculations are done can be found in, for example, [3,4,18]. We considered  $S \rightarrow P$ ,  $S \rightarrow D$ , and  $S \rightarrow F$  atomic transitions for several choices of incoming twisted-photon quantum numbers as labeled in the figures. With exceptions at some values of  $b$ , for  $S \rightarrow P$  transitions the atoms still absorb just one unit of AM into their electronic degrees of freedom, just like for plane

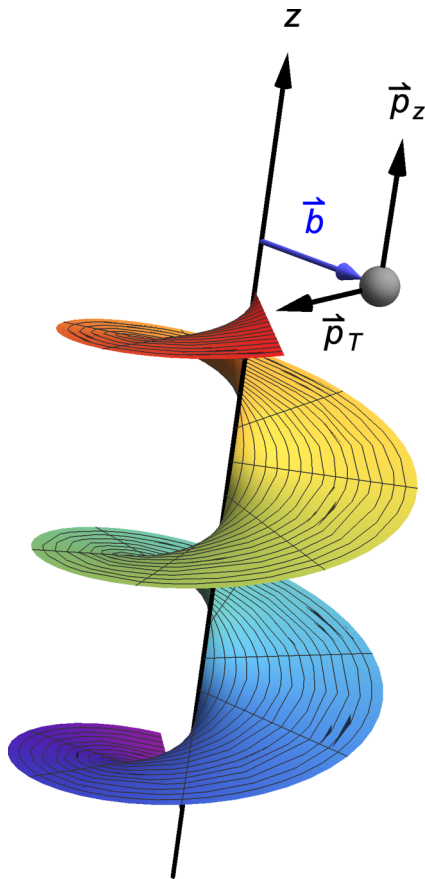


FIG. 1. Twisted photon's helical wavefront (a plane of constant phase for a twisted photon) and an atomic target located at an impact parameter  $b$  from the photon's vortex axis (or phase singularity), here chosen to be the  $z$  axis. The momenta  $p_T$  and  $p_z$  show transverse recoil and longitudinal recoil, respectively.

waves (with  $\Delta m = \pm 1$  dipole selection rules). The rest of the AM must go into c.m. motion. For  $S \rightarrow D$  and  $S \rightarrow F$  transitions, the AM transfers to  $\langle \ell_z \rangle_{\text{c.m.}}$  deviating from plane-wave selection rules for smaller, subwavelength, values of  $b$ , especially when the total incoming photon AM is greater than a single  $\hbar$ . The calculation applies for the case when magnetic quantum numbers of the excited atom are not resolved. There is also a possibility to measure individual transitions into Zeeman sublevels if these levels are split by an external magnetic field, as was done in Refs. [5,6].

The peaks seen in Fig. 2 at  $b/\lambda \approx 4$  are striking and interesting, albeit not the main point of the figure. They occur because, at most values of the impact parameter not near zero, there is one dominant amplitude, whose calculated form contains a Bessel function with argument dependent on the impact parameter. For the  $S \rightarrow P$  transition induced by  $m_\gamma = 1$  and  $\Lambda = 1$ , the dominant amplitude [18] gives  $\langle \ell_f \rangle_{\text{c.m.}} = 0$ , but has a zero at  $b/\lambda \approx 4$ . The subdominant amplitudes then give the observed result. For the case just mentioned, there is just one subdominant amplitude and it gives  $\langle \ell_f \rangle_{\text{c.m.}} = 1$ . For other cases, there are usually two subdominant amplitudes that pull  $\langle \ell_f \rangle_{\text{c.m.}}$  in opposite directions and the interesting peaks are less pronounced.

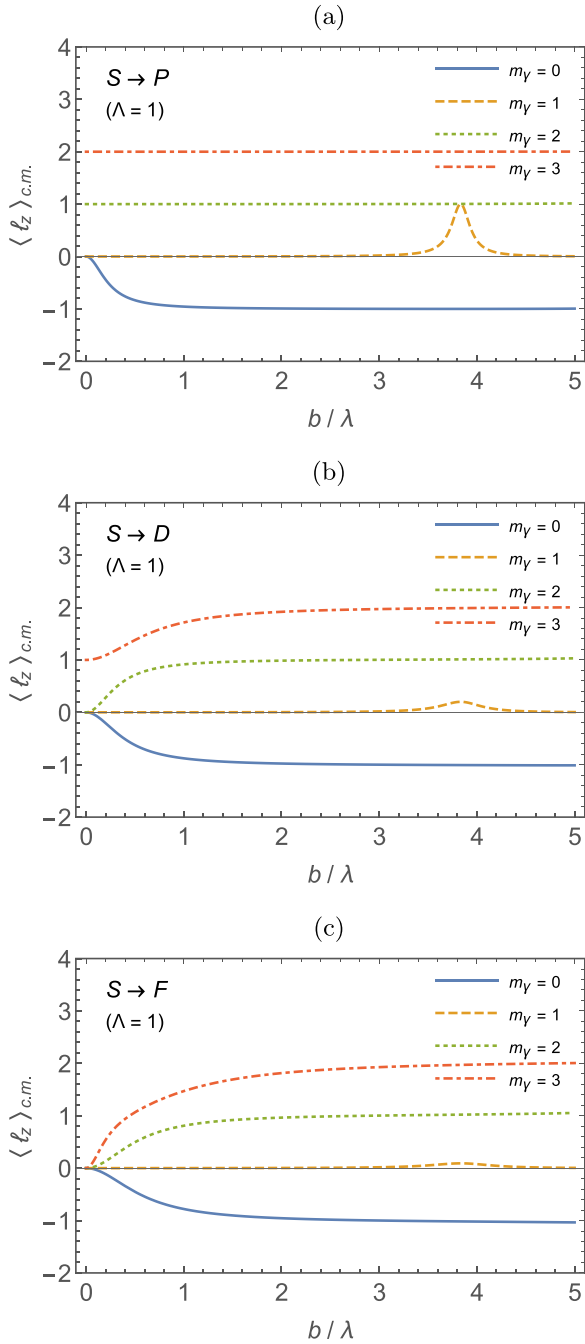


FIG. 2. Mean angular momentum transfer  $\langle \ell_z \rangle_{c.m.}$ , Eq. (1), along the beam direction passed by twisted light of total angular momentum  $m_\gamma$  to an atom's c.m. motion for (a)  $S \rightarrow P$  transitions, (b)  $S \rightarrow D$  transitions, and (c)  $S \rightarrow F$  transitions. For all cases,  $\Lambda = +1$  where  $\Lambda$  is (paraxially) the spin angular momentum of the twisted photon. The horizontal axis shows atom's position  $b$  with respect to the vortex center measured in units of light's wavelength. The figures are for pitch angle [3,18] 0.1 radian. See text for further comments.

While the longitudinal momentum of the atom's recoil equals photon's longitudinal momentum  $p_z = \hbar\omega/c$  (in the paraxial approximation, and where  $\omega$  is photon's angular frequency), the transverse recoil momentum  $p_T$  can be evaluated through AM conservation as  $p_T = \langle \ell_z \rangle_{c.m.}/b$  (at least for

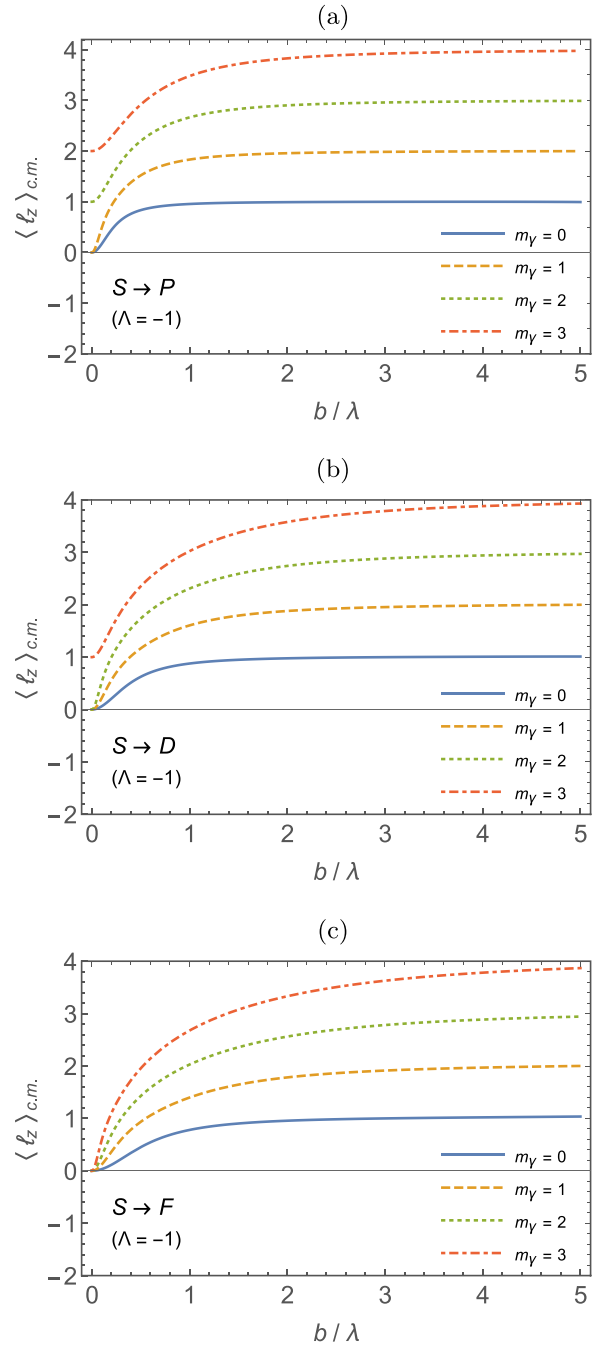


FIG. 3. Same as Fig. 2, but for  $\Lambda = -1$ .

values of  $b$  well larger than the radius of the target [8]). Therefore their ratio is

$$\frac{p_T}{p_z} = \frac{\langle \ell_z \rangle_{c.m.} \lambda}{2\pi\hbar} \frac{\lambda}{b}, \quad (3)$$

where  $\lambda$  is twisted-photon's wavelength.

For the case in which photon's spin ( $\Lambda$ ) and total AM ( $m_\gamma$ ) are aligned, and the atomic transition is  $S \rightarrow P$ , as shown in Fig. 2(a), the orbital AM is given by  $\langle \ell_z \rangle_{c.m.} = \hbar(m_\gamma - \Lambda)$ . We obtain a simple formula for the transverse recoil

momentum,

$$p_T = \hbar \frac{m_\gamma - \Lambda}{b}. \quad (4)$$

It follows that the longitudinal and transverse recoil momenta become equal at the value of impact parameter,

$$b = \lambda \frac{m_\gamma - \Lambda}{2\pi}. \quad (5)$$

However, if some of the excess AM of the incoming twisted photon is passed to internal excitation of the target, then the c.m. recoil is damped at subwavelength distances near the vortex center. This effect is shown for the ratios  $p_T/p_z$  in Figs. 4 and 5. Qualitatively, this effect was discussed in Ref. [19], but specific predictions for nondipole transitions are presented here.

The above results indicate that for  $S \rightarrow P$  transitions [see Fig. 2(a) and 4(a) for  $m_\gamma = 2, 3$ ], the approach of Barnett and Berry [8] to the evaluation of atomic recoil for absorption of the twisted light is justified. They do have general  $m_\gamma$ , but limit consideration to a single level final state and only have dipole transitions. For general cases, modification is required, as shown here.

### B. Twisted-photon absorption on cold trapped ions

Let us consider atomic recoil of a  $^{40}\text{Ca}^+$  ion after absorption of 397 nm photon in an  $S \rightarrow P$  transition or 729 nm photon in an  $S \rightarrow D$  transition that define the “carrier” frequency of the absorbed photons.

In presence of atomic target recoil, energy conservation is modified as follows:

$$\hbar\omega = \hbar\omega_0 + \frac{p_z^2 + p_T^2}{2M}, \quad (6)$$

where  $\hbar\omega_0$  defines the excited energy level.

If, for example, a free ion of  $^{40}\text{Ca}^+$  absorbs a plane-wave photon of wavelength  $\lambda = 397$  nm and energy  $E_\gamma = 3.12$  eV, corresponding to an  $E1$   $S \rightarrow P$  transition, it gives an atom longitudinal recoil energy of  $p_z^2/(2M) = 0.13$  neV, where  $M$  is target’s mass. Twisted-photon absorption generates additional transverse recoil momentum that depends on the impact parameter  $b$  but is independent on photon’s wavelength. Its value can be read from Figs. 4(a) and 5(a). The conversion into transverse recoil energy,  $E_T = p_T^2/(2M)$ , is plotted in Fig. 6, with a comparison line for the longitudinal recoil energy  $p_z^2/(2M)$ . For the  $S \rightarrow D$  electric quadrupole  $E2$  transition at  $\lambda = 729$  nm, the corresponding values of transverse recoil momentum can be read from Figs. 4(b) and 5(b).

In actual experiments, the ions are being held in electromagnetic traps; for example, a segmented Paul trap was used in Refs. [5,6] with RF frequencies of about  $f = \omega_{\text{trap}}^z/2\pi = 1.5$  MHz (along the trap’s  $z$  axis), which corresponds to 6.2 neV energy level spacing in a harmonic oscillator. Different frequencies  $\omega_{\text{trap}}^{x,y}$  describe transverse motion of ions in the trap. From the above, we can estimate the value of impact parameter  $b = 10$  nm for which the transverse recoil equals the energy level spacing of the trap. It affects the Lamb-Dicke parameter  $\eta$  that is crucial for determining ion behavior in the trap. It can be obtained from  $\eta = \sqrt{E_{\text{rec}}/\hbar\omega_{\text{trap}}}$ , where  $E_{\text{rec}}$  is the recoil energy. The condition  $\eta \ll 1$  defines a Lamb-Dicke

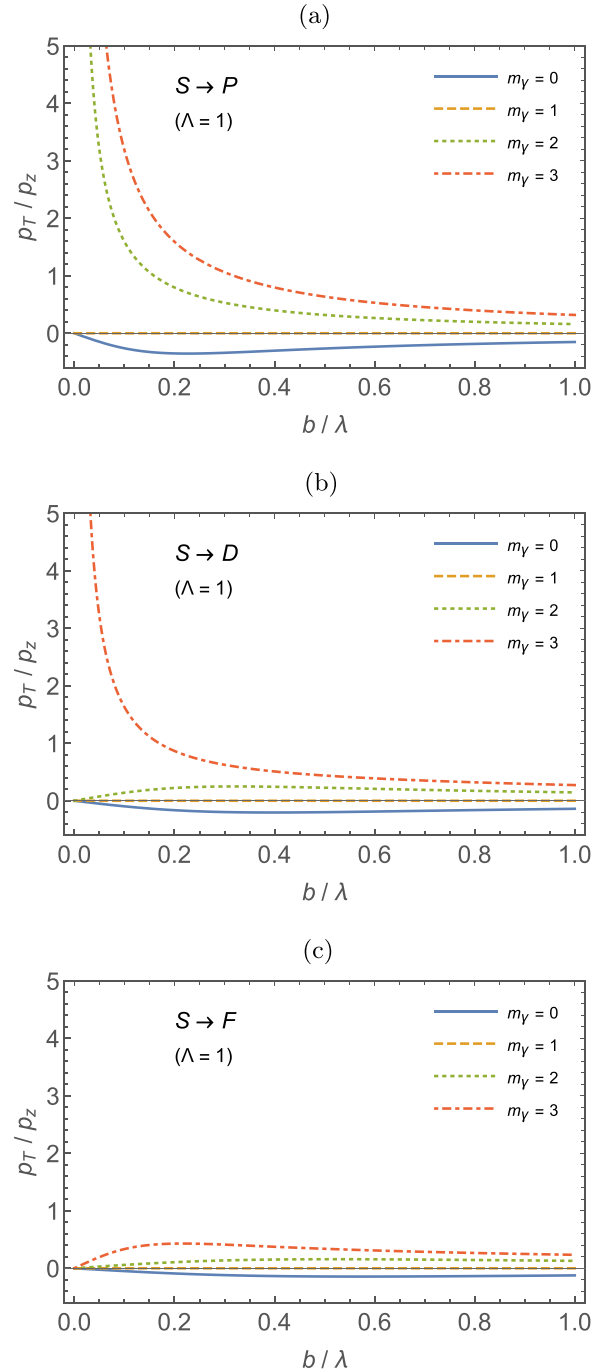
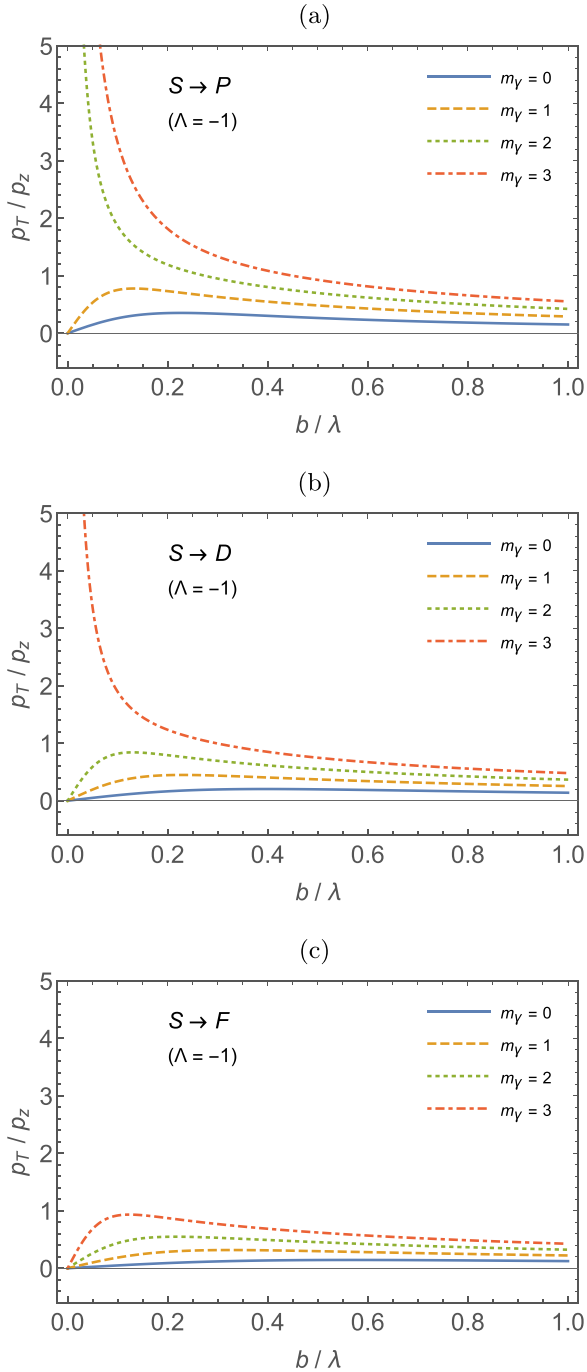


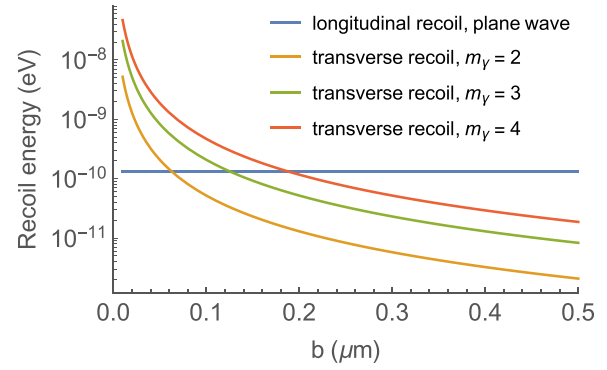
FIG. 4. Ratio of transverse to longitudinal recoil momentum of a free atomic target after absorbing a twisted photon in  $S \rightarrow P$  transition. (a)  $S \rightarrow D$  transition (b) and  $S \rightarrow F$  transition. For all cases,  $\Lambda = +1$ , i.e., the spin of a twisted photon is aligned with its orbital AM. The horizontal axis shows atom’s position  $b$ .

regime important for cooling the ions down to the oscillator ground energy of the trap (see Ref. [20] for details). It implies that the superkick generating  $E_{\text{rec}} \approx \hbar\omega_{\text{trap}}$  results in breaking of a Lamb-Dicke regime for transverse ion motion at sufficiently small values of the impact parameter, depending on light’s orbital AM and trap’s frequency.

A consequence of the larger Lamb-Dicke parameter, or of the recoil energy, is to move the atom into a higher state of the

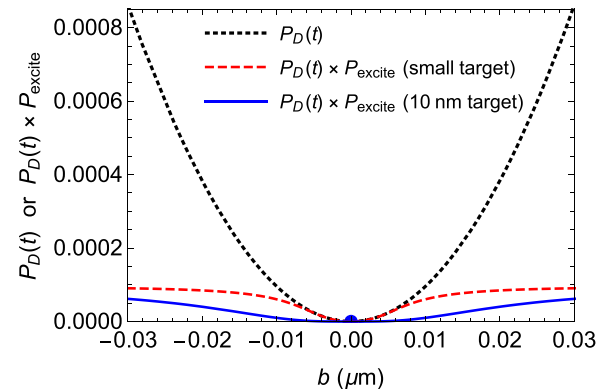
FIG. 5. Same as Fig. 4, but for  $\Lambda = -1$ .

confining potential. Some estimate of how often this happens is shown in Fig. 7, which shows probabilities for exciting a particular transition versus distance of the target atom's wavefunction center from the vortex axis of the beam. The highest curve, a black dotted line, is the full transition probability for this transition, specifically in this case  $S \rightarrow D$  transitions in  ${}^{40}\text{Ca}^+$  with  $m_y = -2$ , the initial state with electron spin projection  $-1/2$ , the final state having magnetic quantum number  $m_f = -3/2$  (i.e., a final atomic electronic state with orbital projection  $\ell_z = -1$ ), and a measurement time of  $26 \mu\text{s}$  [6]. The calculation was done using methods detailed in [6], and

FIG. 6. Recoil energy as a function of impact parameter for longitudinal recoil and transverse recoil at different values of total AM of the absorbed photon,  $\Lambda = 1$ , for  $\lambda = 397 \text{ nm}$   $E1 S \rightarrow P$  transition on  ${}^{40}\text{Ca}^+$  ion.

for larger values of atom-beam separation there is extensive data available [5,6]. One can examine the relevant panel of Fig. 4 of [6] to see the success of the calculation. Technical improvements open the possibility of obtaining data at the narrower atom-beam separations shown here in Fig. 7 [21].

The two other curves in Fig. 7 are the  $S \rightarrow D$  transition probability multiplied by the further probability that the ion will be forced to jump to an excited state of the trapping potential by the transverse kick it receives during the photoexcitation. Both curves are for a trap with the harmonic oscillator potential alluded to earlier, which has a level spacing of 6.2 neV, which in turn gives a ground state wave function proportional to  $\exp(-r^2/2a^2)$ , where the RMS excursion of the wave function in each of the Cartesian coordinates is  $y_{\text{rms}} = a/\sqrt{2}$ . For  ${}^{40}\text{Ca}^+$  and the level spacing given,  $y_{\text{rms}} \approx 10 \text{ nm}$ .

FIG. 7. The black dotted curve shows the probability  $P_D(t)$  for an  $S_{1/2} \rightarrow D_{5/2}$  transition, specifically for  $m_y = -2$ ,  $m_i = -1/2$ ,  $m_f = -3/2$ , and a measurement time of  $26 \mu\text{s}$  (the same as for the data for the same transition in [6]). Also shown is the transition probability multiplied by the further probability that the atom is put into an excited state in its trapping potential by the linear transverse kick. The latter is shown for two cases: a red dashed line for an atom with an almost pointlike spatial distribution, and a blue solid line for a realistic case in which an atom is spread over some region in a harmonic oscillator potential, in this case, with a 10 nm RMS spread. In this plot,  $b$  is the displacement of the target atom location leftward or rightward relative to the beam axis, along a horizontal direction.

For a very small target located at impact parameter  $b$ , the transverse momentum kick would be

$$p_{\perp} = \frac{m_{\gamma} - \ell_z}{b}. \quad (7)$$

However, the actual target is spread over a larger, albeit still not very large, and experimentally realizable region. In the latter case, the superkick is reduced because the atom's wave function in the confining potential can straddle the vortex line. If the target is centered at  $b$  and has a Gaussian c.m. wave function with RMS spread as above, one can use methods analogous to [8] to obtain a transverse kick,

$$p_{\perp} = (m_{\gamma} - \ell_z) \frac{b}{a^2 + b^2}. \quad (8)$$

Of course, the atom is still in the trapping potential, so the superkick will not free it, but can make the c.m. wave function jump to an excited state of the potential. With a harmonic oscillator potential, the probability of finding the c.m. motion in an excited state is the complement of finding it still in the ground state, and modeling it with harmonic oscillator wave functions and the momentum kick just given, one has

$$P_{\text{excite}} = 1 - \exp\left(-\frac{a^2 p_{\perp}^2}{2}\right). \quad (9)$$

Figure 7 shows the result for the 10 nm case in solid blue, and the idealized case where the atom gets the small target momentum transfer in dashed red.

The calculation and Fig. 7 show that there is a jump to an excited state for about one transition in 15 due to the linear superkick, which could be enough to see, if one can do measurements at small impact parameters. It should be noted that the shift in absorption energy is a position-dependent combined effect of c.m. motion of the oscillator and internal rotation of the oscillator. If the twisted-photon beam is aligned along the trap's  $z$  axis, and the trap's confining potential is isotropic in the  $x, y$  directions ( $\omega_{\text{trap}}^{x,y} = \omega_{\text{trap}}^T$ ), then the superkick effect will result in emerging sidebands at energies shifted by  $\pm\omega_{\text{trap}}^T$ . The relative strength of these sidebands with respect to the main "carrier" frequency of the atomic transition depends on the impact parameter  $b$ , the width of trapped ion's wave packet, and whether or not the transverse motion is in the ground state (for which red-shifted sideband  $-\omega_{\text{trap}}^T$  is not allowed). For the beam centered on the trapped ion's wave packet, the twisted-photon absorption results in either red or blue shift of absorbed photons, and disappearance of the "carrier" frequency absorption line.

We add a few comments. Ion cooling in optical molasses produced by twisted light for the purposes of quantum computing and/or precision fundamental measurements was discussed in the literature, with a proposal in Ref. [22] to use polarization gradients formed in the superposition of the twisted light beams. (For more discussions and approaches, see review [19].) Here, we emphasize that for ions located at  $b \leq \lambda(m_{\gamma} - \Lambda)/2\pi$  the transverse recoil in electric-dipole single-photon absorption may exceed longitudinal recoil, and this fact has to be taken into account in possible ion-cooling scenarios.

Due to increased transverse recoil of the trapped ions, the corresponding Lamb-Dicke parameters will be increased in

the vicinity of the optical vortex center, which may affect both Doppler cooling and sideband cooling processes [20] required for quantum computing and precision measurements. Experimental observation of the change in laser cooling dynamics of trapped ions can potentially provide a method to study the superkick effect.

Finally, we point out the fact that the transverse recoil passed to the trapped ions can generate quantized 3D motion characterized by discrete values of orbital AM. It may offer new opportunities for quantum state manipulation in quantum computing applications.

### C. Photodisintegration of deuterium

Let us now consider one of the simplest photonuclear processes, photodisintegration of a deuteron,

$$\gamma + D \rightarrow n + p, \quad (10)$$

where the symbols  $D$ ,  $n$ , and  $p$  stand for deuteron, neutron, and proton, respectively. The deuteron's binding energy is known with sub-keV accuracy,  $E_B = 2224.570 \pm 0.001$  keV [23]. Since the binding energy is much smaller than deuteron's mass, we can use Eq. (6) to evaluate the reaction threshold. Like in the case of ion excitation, in the dipole ( $M1, E1$ ) transitions that dominate near the threshold [24], the transverse recoil momentum depends on deuteron's position and increases toward smaller values of impact parameter  $b$ . For plane-wave incident photons with wavelength  $\lambda = 559$  fm, the recoil energy at the threshold is  $E_B^2/2Mc^2 = 1.3$  keV, which is much larger than the current 1 eV error in deuteron's binding energy. For the twisted photons providing one extra unit of AM to c.m. motion of the final neutron-proton state, the recoil energy would double to 2.6 keV for  $b = \lambda/2\pi = 89$  fm and would increase as  $1/b^2$  for smaller values of  $b$  until the uncertainty in deuteron's spatial location becomes a limiting factor. The probability of this reaction due to twisted photons in the dipole approximation was considered in Ref. [25]; we point out here that for the same approximation the reaction threshold is increased as a function of nucleus's position with respect to the vortex axis of a twisted photon.

Would it mean that the reaction threshold is modified overall for the above reaction? The answer is "not always", because another allowed transition near the threshold is electric quadrupole ( $E2$ ) into the triplet  $^3S_1$  state of unbound neutron and proton, which is due to a relatively small,  $\approx 5\%$  admixture of  $D$  state in the deuteron's wave function. If the twisted photon's total AM equals  $m_{\gamma} = 2\hbar$ , in  $E2$  transition the target would absorb this AM into its intrinsic degrees of freedom, and not in c.m. motion, the extra recoil would be the same as in the plane-wave photon case and the threshold for  $E2$  transition remains unchanged in the vicinity of the vortex center. However, for higher values of  $m_{\gamma}$ , the threshold energy must also be increased, although with a larger phase space for quadrupole transitions than for dipole ones. Independently, the matrix elements of quadrupole transitions can also be enhanced compared to dipole due to novel AM selection rules in the twisted-photon absorption (see Ref. [26,27]).

A possible way to observe the superkick in this photonuclear process would be through analysis of the energy spectrum of final protons and/or neutrons. For kinematics

near the reaction threshold, the neutron-proton pair is produced with a small relative momentum and moves almost parallel to the incident photon. Since the additional recoil momentum from twisted  $\gamma$  rays is purely transverse, measuring energies of either of the nucleons emerging at large angles (with respect to the beam) and having an energy excess would indicate the superkick effect; the excess recoil energy can be measured by proton or neutron spectrometry or time-of-flight methods. If observed, these nucleons with  $\gtrsim$  keV energy excess would pinpoint the spatial location of the reaction to a hundred of femtometers within the phase singularity of the twisted  $\gamma$  ray.

Tight focusing of twisted gamma-ray beams is essential for the feasibility of such measurements. We estimate that if the beam is focused to about 50 picometers, then approximately one percent of final nucleons would have transverse momenta exceeding one-tenth of their longitudinal momentum. If, however, the beam is focused within 3 picometers, then the number of such nucleons reaches 99 percent.

The above findings imply that for a range of twisted-photon energies near the threshold of deuteron photodisintegration, one can observe a complete absence of  $E1$  or  $M1$  transitions, while the only surviving transitions will be electric quadrupole  $E2$ , sensitive to deuteron's  $D$ -state admixture known to be a fundamental property of nucleon-nucleon interactions in need to precision determination. Thus, twisted photons may become a new tool for nuclear physics studies; a possibility of their generation for nuclear studies via Compton backscattering, or inverse Thompson scattering, was discussed in Refs. [28,29].

### III. SUMMARY

We have demonstrated that twisted-photon absorption in several examples of quantum processes leads to additional recoil momentum of the final particles. Overall, it leads to increased threshold energy required for the process to occur. The increase of threshold energy depends on the impact parameter, or the location of the interaction region with respect to the vortex axis of a twisted particle, which implies subwavelength position resolution for corresponding measurement.

The excess recoil is small albeit measurable for atomic and nuclear photoinduced reactions at eV and MeV energies.

We can extend our discussion by noting that the size of the superkick depends on the distance from the vortex line to the interaction region. To be able to speak of such a distance requires that the interactions region be localizable and small. In the examples we have studied so far, the requirement is satisfied by having a localized target.

It is possible to satisfy the need for localization with a broader target and producing the final state within a localized production volume. For example, consider electromagnetic lepton pair production, as  $\gamma\gamma \rightarrow e^+e^-$ , where one initial photon is very high energy (VHE) and twisted and the other is ordinary and lower energy, perhaps even ambient light. The  $e^+e^-$  production, in a Feynman diagram expansion, requires internal electron lines off-shell by an electron mass or more, limiting the propagation region range in coordinate space. The electron and positron must emerge from a common interaction region with a spatial scale of about a Compton wavelength, or about 2.4 picometers.

To make the possibilities more concrete, a 100 GeV VHE plane wave photon hitting a 2.5 eV, or green visible light, the photon is just at the threshold for producing an  $e^+e^-$  pair. For a twisted photon, there will be impact parameter dependent modifications of the threshold energy, and the need for the impact parameter to be about a Compton wavelength or greater to avoid the production region straddling the vortex line is a serious but not conclusive consideration. However, further study of observable superkick phenomena with final state rather than initial state localization is deferred to future work.

### ACKNOWLEDGMENTS

The work of A.A. was supported by US Army Research Office Grant No. W911NF-19-1-0022. C.E.C. thanks the National Science Foundation (USA) for support under Grant No. PHY-1812326. A.A. thanks Michael Berry for stimulating discussions of the “superkick” during ICOAM'17 conference. Discussions with Ferdinand Schmidt-Kaler and Christian Schmiegelow on physics of cold trapped ions are also gratefully acknowledged.

---

- [1] D. L. Andrews and M. Babiker (eds.), *The Angular Momentum of Light* (Cambridge University Press, Cambridge, 2013).
- [2] S. Franke-Arnold and N. Radwell, Light served with a twist, *Opt. Photonics News* (2017).
- [3] A. Afanasev, C. E. Carlson, and A. Mukherjee, Off-axis excitation of hydrogenlike atoms by twisted photons, *Phys. Rev. A* **88**, 033841 (2013).
- [4] H. M. Scholz-Marggraf, S. Fritzsche, V. G. Serbo, A. Afanasev, and A. Surzhykov, Absorption of twisted light by hydrogenlike atoms, *Phys. Rev. A* **90**, 013425 (2014).
- [5] C. T. Schmiegelow, J. Schulz, H. Kaufmann, T. Ruster, U. G. Poschinger, and F. Schmidt-Kaler, Transfer of optical orbital angular momentum to a bound electron, *Nat. Commun.* **7**, 12998 (2016).
- [6] A. Afanasev, C. E. Carlson, C. T. Schmiegelow, J. Schulz, F. Schmidt-Kaler, and M. Solyanik, Experimental verification of position-dependent angular-momentum selection rules for absorption of twisted light by a bound electron, *New J. Phys.* **20**, 023032 (2018).
- [7] S. M. Barnett, On the quantum core of an optical vortex, *J. Mod. Opt.* **55**, 2279 (2008).
- [8] S. M. Barnett and M. V. Berry, Superweak momentum transfer near optical vortices, *J. Opt.* **15**, 125701 (2013).
- [9] M. Babiker, C. R. Bennett, D. L. Andrews, and L. C. Dávila Romero, Orbital Angular Momentum Exchange in the Interaction of Twisted Light with Molecules, *Phys. Rev. Lett.* **89**, 143601 (2002).

[10] A. Afanasev, C. E. Carlson, and A. Mukherjee, Two properties of twisted-light absorption, *J. Opt. Soc. Am. B* **31**, 2721 (2014).

[11] M. Berry *et al.*, Roadmap on superoscillations, *J. Opt.* **21**, 053002 (2019).

[12] G. Yuan, E. T. F. Rogers, and N. I. Zheludev, Plasmonics in free space: Observation of giant wavevectors, vortices, and energy backflow in superoscillatory optical fields, *Light Sci. Appl.* **8**, 2 (2019), arXiv:1805.11794 [physics.optics].

[13] E. T. F. Rogers, S. Quraish, K. S. Rogers, T. A. Newman, P. J. S. Smith, and N. I. Zheludev, Far-field unlabeled super-resolution imaging with superoscillatory illumination, *APL Photonics* **5**, 066107 (2020).

[14] I. P. Ivanov, N. Korchagin, A. Pimikov, and P. Zhang, Doing Spin Physics With Unpolarized Particles, *Phys. Rev. Lett.* **124**, 192001 (2020).

[15] I. P. Ivanov, N. Korchagin, A. Pimikov, and P. Zhang, Kinematic surprises in twisted-particle collisions, *Phys. Rev. D* **101**, 016007 (2020).

[16] A. Afanasev, C. E. Carlson, and A. Mukherjee, High-multipole excitations of hydrogen-like atoms by twisted photons near a phase singularity, *J. Opt.* **18**, 074013 (2016).

[17] The probabilities  $w(m_f)$  are proportional to the transition amplitudes that can, for example, be found in Eq. (6) or Eq. (18) of [18], and normalized so they sum to unity. [For Figs. 2 and 3 when  $|m_\gamma| > l_f$ , the  $b = 0$  point (only) should be omitted, since all transition amplitudes are zero in that case. For  $b \neq 0$ , all curves are valid, and for  $|m_\gamma| \leq l_f$  the  $b = 0$  point is also valid.].

[18] A. Afanasev, C. E. Carlson, and H. Wang, Polarization transfer from the twisted light to an atom, *J. Opt.* **22**, 054001 (2020).

[19] M. Babiker, D. L. Andrews, and V. E. Lembessis, Atoms in complex twisted light, *J. Opt.* **21**, 013001 (2018).

[20] J. Eschner, G. Morigi, F. Schmidt-Kaler, and R. Blatt, Laser cooling of trapped ions, *J. Opt. Soc. Am. B* **20**, 1003 (2003).

[21] F. Schmidt-Kaler and C. Schmiegelow (private communication).

[22] V. E. Lembessis, D. Ellinas, and M. Babiker, Azimuthal sisyphus effect for atoms in a toroidal all-optical trap, *Phys. Rev. A* **84**, 043422 (2011).

[23] From CODATA 2018, Values of Fundamental Physical Constants, <https://physics.nist.gov/cuu/Constants/index.html>.

[24] J. M. Blatt and V. Weisskopf, *Theoretical Nuclear Physics* (Springer, New York, 1979).

[25] A. Afanasev, V. G. Serbo, and M. Solyanik, Radiative capture of cold neutrons by protons and deuteron photodisintegration with twisted beams, *J. Phys. G: Nucl. Part. Phys.* **45**, 055102 (2018).

[26] A. Afanasev, C. E. Carlson, and M. Solyanik, Atomic spectroscopy with twisted photons: Separation of  $m1-e2$  mixed multipoles, *Phys. Rev. A* **97**, 023422 (2018).

[27] M. Solyanik-Gorgone, A. Afanasev, C. E. Carlson, C. T. Schmiegelow, and F. Schmidt-Kaler, Excitation of  $e1$ -forbidden atomic transitions with electric, magnetic, or mixed multipolarity in light fields carrying orbital and spin angular momentum, *J. Opt. Soc. Am. B* **36**, 565 (2019).

[28] U. D. Jentschura and V. G. Serbo, Generation of High-Energy Photons with Large Orbital Angular Momentum by Compton Backscattering, *Phys. Rev. Lett.* **106**, 013001 (2011).

[29] V. Petrillo, G. Dattoli, I. Drebot, and F. Nguyen, Compton Scattered X-Gamma Rays with Orbital Momentum, *Phys. Rev. Lett.* **117**, 123903 (2016).